



# Wavelet modulation: An alternative modulation with low energy consumption

Marwa Chafii, Jacques Palicot, Rémi Gribonval

## ► To cite this version:

Marwa Chafii, Jacques Palicot, Rémi Gribonval. Wavelet modulation: An alternative modulation with low energy consumption. *Comptes Rendus. Physique*, 2017, 18 (2), pp.156-167. <10.1016/j.crhy.2016.11.010>. <hal-01445465>

**HAL Id: hal-01445465**

**<https://hal.science/hal-01445465v1>**

Submitted on 30 Jan 2017

**HAL** is a multi-disciplinary open access archive for the deposit and dissemination of scientific research documents, whether they are published or not. The documents may come from teaching and research institutions in France or abroad, or from public or private research centers.

L'archive ouverte pluridisciplinaire **HAL**, est destinée au dépôt et à la diffusion de documents scientifiques de niveau recherche, publiés ou non, émanant des établissements d'enseignement et de recherche français ou étrangers, des laboratoires publics ou privés.



HAL Authorization



Energy and radiosciences / Énergie et radiosciences

## Wavelet modulation: An alternative modulation with low energy consumption

*La modulation en ondelettes : une modulation alternative à faible consommation d'énergie*Marwa Chafii <sup>a,\*</sup>, Jacques Palicot <sup>a</sup>, Rémi Gribonval <sup>b</sup><sup>a</sup> CentraleSupélec, IETR, Campus de Rennes, 35576 Cesson-Sévigné cedex, France<sup>b</sup> IRISA, Inria – Bretagne Atlantique, 35042 Rennes cedex, France

## ARTICLE INFO

## Keywords:

Wavelet modulation  
Wavelet transform  
OFDM  
Peak-to-Average-Power Ratio  
Meyer wavelet  
Haar wavelet

## Mots-clés :

Modulation en ondelettes  
Transformée en ondelettes  
OFDM  
Facteur de crête  
Ondelettes de Meyer  
Ondelette de Haar

## ABSTRACT

This paper presents wavelet modulation, based on the discrete wavelet transform, as an alternative modulation with low energy consumption. The transmitted signal has low envelope variations, which induces a good efficiency for the power amplifier. Wavelet modulation is analyzed and compared for different wavelet families with orthogonal frequency division multiplexing (OFDM) in terms of peak-to-average power ratio (PAPR), power spectral density (PSD) properties, and the impact of the power amplifier on the spectral regrowth. The performance in terms of bit error rate and complexity of implementation are also evaluated, and several trade-offs are characterized.

© 2016 Académie des sciences. Published by Elsevier Masson SAS. This is an open access article under the CC BY-NC-ND license (<http://creativecommons.org/licenses/by-nc-nd/4.0/>).

## R É S U M É

Dans cet article, nous présentons la modulation en ondelettes, basée sur la transformée discrète en ondelettes, comme une modulation à faible consommation d'énergie. Le signal généré par cette modulation a, en effet, de faibles variations de puissance par construction. Nous analysons la modulation en ondelettes pour plusieurs familles d'ondelettes et nous comparons ses performances avec celles de l'OFDM, en termes de facteur de crête (PAPR), de propriétés de la densité spectrale de puissance ainsi que de l'impact de l'amplificateur de puissance sur la remontée des lobes secondaires. Les performances en termes de taux d'erreur binaire et de complexité d'implémentation sont également évaluées, et plusieurs compromis sont caractérisés.

© 2016 Académie des sciences. Published by Elsevier Masson SAS. This is an open access article under the CC BY-NC-ND license (<http://creativecommons.org/licenses/by-nc-nd/4.0/>).

\* Corresponding author.

E-mail addresses: [marwa.chafii@supelec.fr](mailto:marwa.chafii@supelec.fr) (M. Chafii), [jacques.palicot@centralesupelec.fr](mailto:jacques.palicot@centralesupelec.fr) (J. Palicot), [remi.gribonval@inria.fr](mailto:remi.gribonval@inria.fr) (R. Gribonval).

This work is an extended version of our study on the Meyer wavelet modulation, published in the conference papers [1,2]. Compared to [1,2], we present here a more complete study covering other wavelet families and analyzing the power amplifier effect on the spectral regrowth.

## 1. Introduction

In communications, an important effect of the large amplitude variations of the transmitted multicarrier signal is the weak power efficiency of the power amplifier. This causes intensive energy consumption and growing need for cooling. Our objective is to propose an alternative to the classical multicarrier modulations in order to reduce energy consumption.

Orthogonal frequency division multiplexing (OFDM) is a modulation scheme adopted by various wireline and wireless communication standards as a modulation technique for data transmission. However, the OFDM signal suffers from high power fluctuations. The variations of its envelope generate non-linear distortions when we introduce the OFDM signal into a power amplifier (PA). In order to avoid the compression range of the PA and amplify the signal in the linear domain of the PA characteristic, an input back-off (IBO) is performed at the input of the PA. However, when the input back-off gets larger, power efficiency gets poorer, which induces high energy consumption.

PA energy consumption may represent more than 60% of the energy consumption of the LTE macro base-station transmitter [3]. Reducing the envelope variations, and then improving the amplifier's efficiency, contributes to reducing energy consumption at the level of mobile equipments (batteries that last longer), and at the level of the base stations (energy savings and reduced electricity bill for telecom operators). Therefore, this could help the reduction of CO2 emissions and prevent environmental pollution.

The peak-to-average power (PAPR) is a random variable that has been introduced to measure the power variations of the OFDM signal. Much research has been conducted in order to reduce the PAPR and analyze its probability distribution. In our previous work [4], we have studied the complementary cumulative distribution function (CCDF) of the PAPR, and we have shown that it depends on the waveform used in the modulation. The PAPR reduction problem can therefore be formulated as an optimization problem. In [5], we have shown that having a temporal support strictly less than a symbol period is a necessary condition on the waveforms for a better PAPR than OFDM. Since the wavelet basis satisfies this condition, we are interested in exploring wavelet modulation and energy consumption through the evaluation of its PAPR.

In this paper, wavelet modulation is proposed as an alternative modulation with low energy consumption. Power consumption is evaluated through the study of PAPR performance, and compared with that of OFDM. The simulation results show that the proposed scheme for wavelet modulation achieves significant gains in terms of PAPR compared with OFDM, at the cost of affordable increased complexity. A comparison in terms of bit error rate and power spectral density between the OFDM system and the wavelet modulation system is also investigated in this work.

## 2. Wavelet modulation

Wavelets have been applied in several wireless communication applications such as data compression, source and channel coding, signal denoising and channel modeling. Moreover, wavelets have been proposed as a modulation basis for multicarrier modulation systems. The resulting system based on wavelet modulation is often named in the literature as Wavelet-OFDM [6] or also known as orthogonal wavelet division multiplexing (OWDM) [7].

The most common scheme in the literature is wavelet packet modulation (WPM), which is a generalized form of wavelet modulation. WPM has been introduced in the literature by Lindsey [8], who studied the application of the wavelet packet basis in orthogonal multiplexing of data. In this paper, we have chosen to focus on wavelet modulation for its significant PAPR performance gains, as will be studied in Section 3.

### 2.1. Wavelet basis

Let  $\psi$  and  $\phi$  be two functions  $\in L^2(\mathbb{R})$ ,<sup>1</sup> of a finite support<sup>2</sup>  $[0, T_0]$ , such that:

$$\|\psi\|^2 = \|\phi\|^2 = 1 \quad (1)$$

$$\text{and } \int_{-\infty}^{+\infty} \psi(t) dt = 0 \quad (2)$$

The norm  $\|\cdot\|$  of a function  $g \in L^2(\mathbb{R})$  is defined as:  $\|g\|^2 = \int_{-\infty}^{+\infty} |g(t)|^2 dt$ .  $\psi$  and  $\phi$  can be named the mother wavelet function and the mother scaling function respectively.

Let  $L$  be the effective number of scales selected; we define contracted versions  $\psi_j$  and  $\phi_j$  of the functions  $\psi$  and  $\phi$ , for  $j \geq J - L$ ,

<sup>1</sup> The space of square integrable functions.

<sup>2</sup> The support of a function means here the interval outside which the function is equal to zero.

$$\psi_j(t) = 2^{j/2} \psi(2^j t) \quad (3)$$

$$\phi_j(t) = 2^{j/2} \phi(2^j t) \quad (4)$$

The contracted functions  $\psi_j$  and  $\phi_j$  have a support of  $[0, \frac{T_0}{2^j}]$ .

For every scale  $j$ , we define translated versions  $\psi_{j,k}$  and  $\phi_{j,k}$  of the functions  $\psi_j$  and  $\phi_j$  as follows:

$$\psi_{j,k}(t) = \psi_j(t - 2^{-j} k T_0) = 2^{j/2} \psi(2^j t - k T_0) \quad (5)$$

$$\phi_{j,k}(t) = \phi_j(t - 2^{-j} k T_0) = 2^{j/2} \phi(2^j t - k T_0) \quad (6)$$

The contracted translated functions  $\psi_{j,k}$  and  $\phi_{j,k}$  have a support of  $[\frac{k T_0}{2^j}, \frac{(k+1) T_0}{2^j}]$ . For  $j \in \llbracket J-L, J-1 \rrbracket$  and  $k \in \llbracket 0, 2^j - 1 \rrbracket$ , we define the wavelet basis as:

$$\{\phi_{J-L,k}\}_{k=0}^{2^{J-L}-1} \bigcup_{j=J-L}^{J-1} \{\psi_{j,k}\}_{k=0}^{2^j-1} \quad (7)$$

where  $J$  is the number of scales considered.

## 2.2. Expression of the transmitted signal

Wavelet modulation is a multicarrier modulation system based on the wavelet basis instead of the Fourier basis. The modulation system  $\{g_m\}_{m \in \llbracket 0, M-1 \rrbracket}$  is represented by the wavelet functions  $\{\psi_{j,k}\}_{j \in \llbracket J-L, J-1 \rrbracket, k \in \llbracket 0, 2^j-1 \rrbracket}$  and the scaling functions  $\{\phi_{J-L,k}\}_{k \in \llbracket 0, 2^{J-L}-1 \rrbracket}$  of the first scale. The waveforms  $\{g_m\}_{m \in \llbracket 0, M-1 \rrbracket}$  can be expressed as:

$$\{g_m\}_{m \in \llbracket 0, 2^{J_0+1}-1 \rrbracket} := \{\psi_{J_0,k}\}_{k \in \llbracket 0, 2^{J_0}-1 \rrbracket} \cup \{\phi_{J_0,k}\}_{k \in \llbracket 0, 2^{J_0}-1 \rrbracket}$$

$$\{g_m\}_{m \in \llbracket 2^{J_0+1}, 2^J-1 \rrbracket} := \{\psi_{j,k}\}_{j \in \llbracket J_0, J-1 \rrbracket, k \in \llbracket 0, 2^j-1 \rrbracket}$$

The transmitted signal based on wavelet modulation is then defined as follows:

$$x(t) = \sum_n \sum_{j=J-L}^{J-1} \sum_{k=0}^{2^j-1} w_{j,k} \psi_{j,k}(t - n T_0) + \sum_n \sum_{q=0}^{2^{J-L}-1} a_{J-L,q} \phi_{J-L,q}(t - n T_0) \quad (8)$$

- $J-1$ : last scale considered, with  $M = 2^J$ ,
- $L$ : effective number of scales considered ( $J-L \leq j \leq J-1$ ),
- $w_{j,k}$ : wavelet coefficients located at  $k$ -th position from the scale  $j$ ,
- $a_{J-L,k}$ : approximation coefficients located at the  $k$ -th position from the first scale  $J-L$ ,
- $\psi_{j,k} = 2^{j/2} \psi(2^j t - k T_0)$ : the wavelet orthogonal functions,
- $\phi_{J-L,k} = 2^{\frac{J-L}{2}} \phi(2^{J-L} t - k T_0)$ : the scaling orthogonal functions at the scale  $J-L$ .

The mother wavelet function and the mother scaling function correspond to  $j=0, k=0$ . To each scale  $j$  corresponds  $2^j$  translated wavelet functions. From one scale to the next, the number of wavelet functions is then multiplied by two.

## 2.3. Variants

Several variants of wavelet modulation can be considered, depending on the number of scales  $L$  selected. Since the scaling functions are considered only for the first scale,  $J-L$  then defines the number of the scaling functions  $\phi_{j,k}$  in the modulation system. Fig. 1 depicts the wavelet modulation system for different values of  $L$ , for  $M = 8$  carriers. By convention, when  $L = 0$ , there are  $2^J$  scaling functions  $\phi_{j,k}$  and no wavelet function  $\psi_{j,k}$  considered in the wavelet basis (the case of single carrier modulation).

Note that the position of the functions in Fig. 1 is not a coincidence, but it has an importance, since it gives an idea about the time-frequency localization of the waveforms  $(\Delta t, \Delta f)$ .

## 2.4. Some wavelets

In this section, we outline some important wavelet families: Meyer wavelets, which allow compact frequency support, and Daubechies wavelets, which are characterized by a compact temporal support.

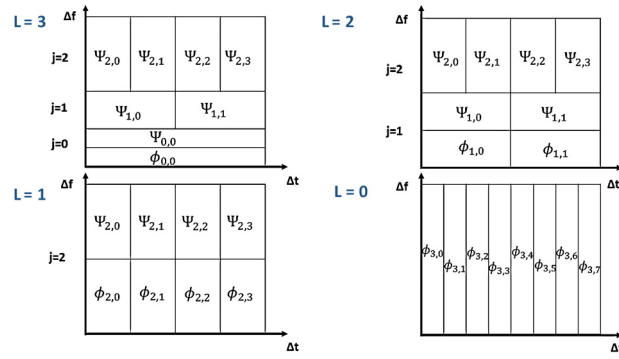
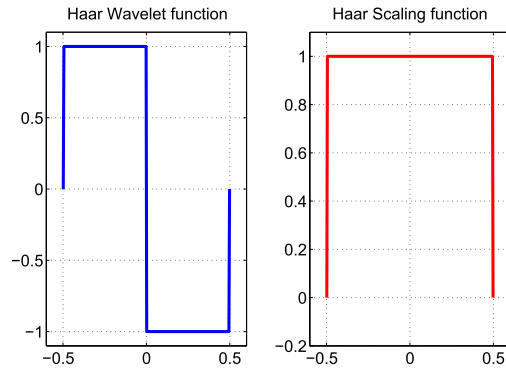
Fig. 1. Some variants of wavelet modulation for  $M = 8$ .

Fig. 2. Haar mother wavelet and scaling function.

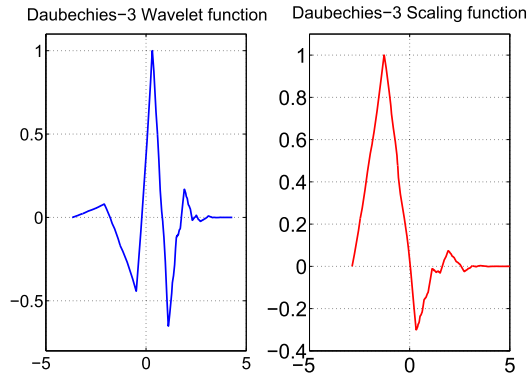


Fig. 3. Daubechies-3 mother wavelet and scaling function.

**Haar wavelet** The Haar wavelet is the oldest and simplest wavelet, and has a closed form expression in the time and frequency domains. The mother Haar wavelet and the mother Haar scaling function are presented in Fig. 2, and are expressed as follows:

$$\psi(t) = \begin{cases} \frac{1}{\sqrt{T_0}} & \text{if } 0 \leq t \leq \frac{T_0}{2} \\ -\frac{1}{\sqrt{T_0}} & \text{if } \frac{T_0}{2} \leq t \leq T_0 \\ 0 & \text{else} \end{cases} \quad (9)$$

$$\phi(t) = \begin{cases} \frac{1}{\sqrt{T_0}} & \text{if } 0 \leq t \leq T_0 \\ 0 & \text{else} \end{cases} \quad (10)$$

**Daubechies wavelets** The Daubechies- $p$  wavelets are characterized by a number  $p$  of zero moments. They have compact support and therefore are calculated from conjugate mirror filters  $f^l$  of finite impulse response [9]. In particular, when  $p$  is

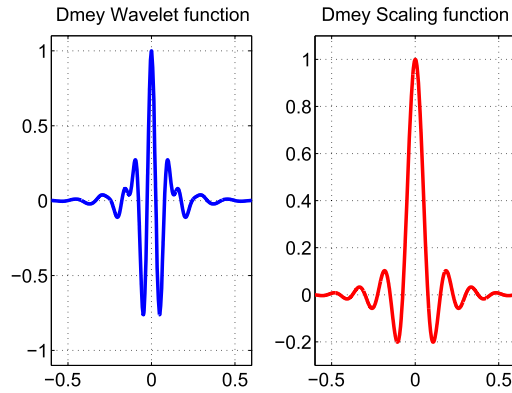


Fig. 4. Dmey mother wavelet and scaling function.

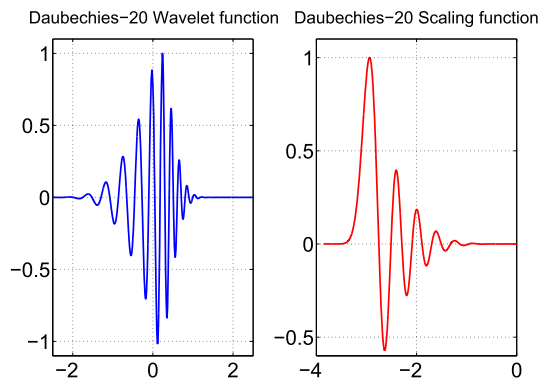


Fig. 5. Daubechies-20 mother wavelet and scaling function.

equal to 1, we get the Haar wavelet. Fig. 3 and Fig. 5 display the functions  $\phi$  and  $\psi$  for  $p = 3$  and  $p = 20$ : Daubechies-3 (db3) and Daubechies-20 (db20).

**Meyer wavelet** The Meyer wavelet is a frequency-band-limited orthogonal wavelet, which has been proposed by Yves Meyer in 1985 [10,11]. Meyer wavelets are indefinitely differentiable orthonormal wavelets, which are well localized and decay from their central peak faster than any inverse polynomial. Dmey is a discrete format approximation of the Meyer wavelet, and it can approximate the Meyer wavelet based on a finite impulse response (FIR) filter, as depicted in Fig. 4.<sup>3</sup> As a result, the fast wavelet transform can approximate the Meyer wavelet transform, and the discrete wavelet transform (DWT) can be applied.

### 3. PAPR performance

A comparison in terms of PAPR performance is presented in Fig. 6 and Fig. 7 for the wavelet modulation variants  $L = 1$  and  $L = 7$  respectively. To evaluate the PAPR performance, the complementary cumulative distribution function (CCDF) of the PAPR is simulated, which is the probability that the PAPR exceeds a defined value  $\gamma$ . The simulation settings consider a number of carriers  $M = 128$  ( $J = 7$ ) and the 16-QAM (quadrature amplitude modulation) constellation.

Different wavelets are selected: the Haar wavelet, the Daubechies wavelets 3 and 20, and the Dmey wavelet. The CCDF for different wavelets are shifted to the left compared with that of OFDM. Therefore, wavelet modulation achieves better PAPR performance than OFDM as summarized in Table 1. In particular, the Haar wavelet reaches the best performance. Intuitively, the PAPR performance gain can be explained by the fact that in wavelet modulation, only  $L$  carriers are overlapping in the same instant, which does not promote the addition of the large peak power.

Following the same reason, the  $L = 1$  variant achieves better PAPR performance than the  $L = 7$  variant. When the number of overlapping carriers  $L$  gets smaller, the PAPR performance gets then better. This can also be interpreted by the consideration that in every decomposition level, the multicarrier system can be seen as a single carrier system, because the

<sup>3</sup> Generated using the MATLAB wavefun('dmey') command.

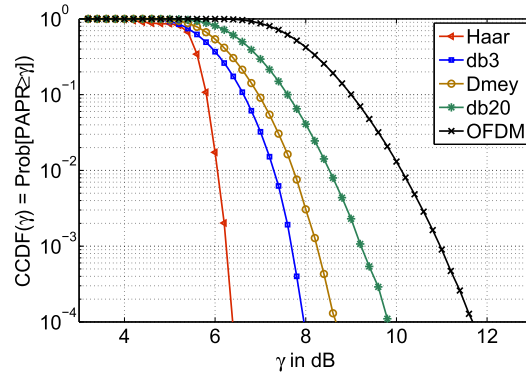


Fig. 6. PAPR performance comparison for  $L = 1$  and  $J = 7$  ( $M = 128$ ).

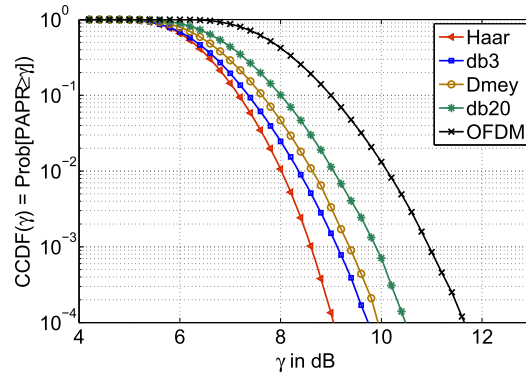


Fig. 7. PAPR performance comparison for  $L = 7$  and  $J = 7$  ( $M = 128$ ).

Table 1

PAPR performance of wavelet modulation compared with OFDM for the 16-QAM constellation.

Wavelet name	Haar	Daubechies-3	Dmey	Daubechies-20
PAPR Gain compared with OFDM at $\text{CCDF} = 10^{-3}$ for $L = 1$ and $J = 7$ ( $M = 128$ )	4.7 dB	3.3 dB	2.8 dB	1.8 dB
PAPR Gain compared with OFDM at $\text{CCDF} = 10^{-3}$ for $L = 7$ and $J = 7$ ( $M = 128$ )	2.4 dB	1.9 dB	1.6 dB	1.1 dB

waveforms of the same scale  $j$  have the same bandwidth and are only shifted in time. As the single carrier system does not suffer from increased PAPR, the smaller  $L$  gets, the less the effect of the PAPR is observed.

Thus, we can conclude that the PAPR performance of wavelet modulation depends on the variant considered and the wavelet family selected. Moreover, all the wavelet modulation schemes achieve better PAPR performance than OFDM. In other words, it can be stated that wavelet modulation consumes less energy than the Fourier functions used in the OFDM system.

#### 4. PSD performance

PSD is a relevant criterion in the evaluation of the spectral efficiency of a modulation scheme. It highlights the main properties of the used bandwidth and the side lobe effects that characterize bandwidth efficiency and adjacent channel interference. In this section, we compare the PSD performance of different wavelet modulation with the OFDM scheme, before and after the power amplifier.

##### 4.1. PSD performance comparison

PSDs for different wavelets are displayed in Figs. 8, 9, 10, and 11 as functions of a normalized frequency, and compared with OFDM. PSD is simulated using Matlab, and estimated via the periodogram method with a rectangular window. Before applying wavelet modulation based on the inverse discrete wavelet transform (IDWT), zero padding by a factor of 4 is performed on the input signal in the frequency domain. The number of carriers considered in the simulations is  $M = 128$  ( $J = 7$ ) and the variant used is  $L = 1$ .

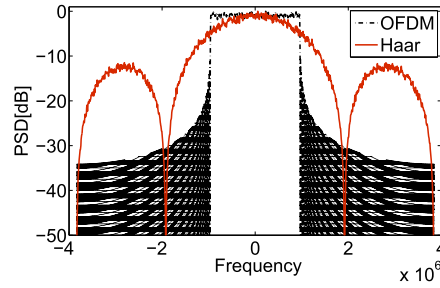


Fig. 8. PSD of Haar wavelet modulation.

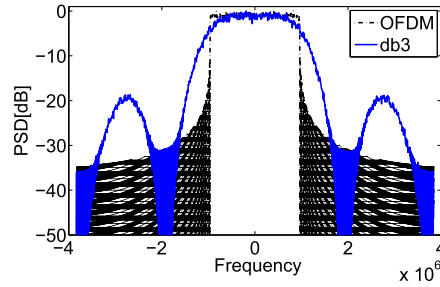


Fig. 9. PSD of Daubechies-3 wavelet modulation.

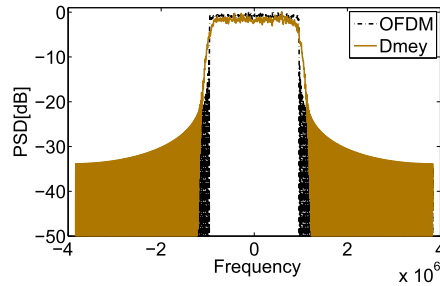


Fig. 10. PSD of Dmey wavelet modulation.

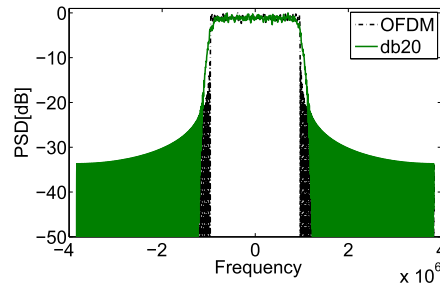


Fig. 11. PSD of Daubechies-20 wavelet modulation.

The most striking observation is the properties of PSD Haar wavelet. The width of the main lobe of its PSD is the double of that of OFDM. Moreover, it suffers from very large side lobes. Many applications can not tolerate these poor spectrum characteristics. It is true that Haar can be filtered to reduce the side lobes effect, but this will change the system's performance. Similarly, the Daubechies-3 wavelet shows significantly degraded PSD performance. In contrast, Dmey and Daubechies-20 wavelets achieve almost comparable performance to that of OFDM.

Haar and Daubechies-3 reach the best PAPR performance as discussed in Section 3, and yet, present the poorest spectrum characteristics. The choice of a suitable wavelet is limited by the trade-off between PAPR performance and PSD properties.

Hereafter, Dmey and Daubechies-20 wavelets are selected to be studied and evaluated for further performances.



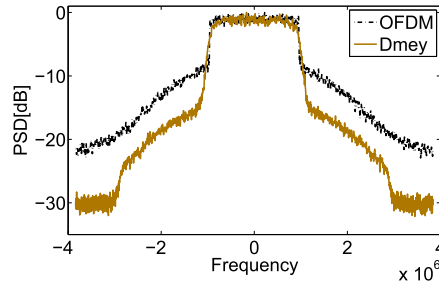


**Fig. 12.** PSD Comparison between Dmey wavelet modulation and OFDM at the output of the power amplifier of the Saleh model.

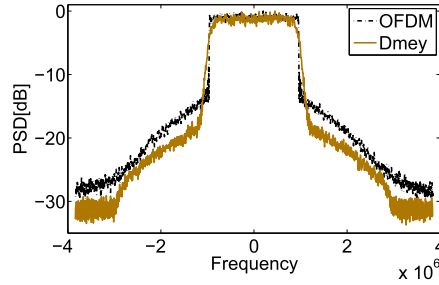


**Fig. 13.** PSD Comparison between Dmey wavelet modulation and OFDM at the output of the power amplifier of the Rapp model.

#### 4.2. Power amplifier effect

In this part, we evaluate the effect of a power amplifier on the PSD properties. We introduce the OFDM signal, the Dmey wavelet modulation signal, and the Daubechies-20 wavelet modulation signal into memoryless power amplifiers based on Saleh's model [12] and Rapp's model [13]. The same simulation parameters of Section 4.1 are considered in this section. The input back-off considered in Saleh's model is 5 dB, while it is fixed at 0 dB for Rapp's model. The relationship between the input and output voltages is usually expressed by the AM/AM function. The AM/PM function characterizes the phase shift between the input and output voltages as a function of the input voltage. The AM/AM and AM/PM functions of Saleh's amplifier model are defined as follows:

$$F_{AM/AM} = \frac{\alpha_a |x(t)|}{1 + \beta_a |x(t)|^2}, \quad F_{AM/PM}(|x(t)|) = \frac{\alpha_p |x(t)|^2}{1 + \beta_p |x(t)|^2} \quad (11)$$

where  $\alpha_a = 2.1587$  and  $\beta_a = 1.1517$  ( $\alpha_p = 4.0033$  and  $\beta_p = 9.1040$ , respectively) are used to compute the amplitude gain (the phase change respectively) for an input signal  $x(t)$ .

The AM/AM function for the Rapp's amplifier model is given by:

$$F_{AM/AM} = \frac{|x(t)|}{\left(1 + \left(\frac{|x(t)|}{O}\right)^{2S}\right)^{1/2S}} \quad (12)$$

where  $|x(t)|$  is the magnitude of the input signal,  $S = 0.5$  is the smoothness factor, and  $O = 1$  is the output saturation level.

As depicted in Figs. 12–15, OFDM faces a spectral regrowth compared with the other wavelets, due to its high PAPR. The spectral regrowth is caused by the non-linearity of the amplifier. When a modulated signal with large envelope fluctuations is introduced into the non-linear amplifier, its bandwidth is broadened due to the non-linearities that generate mixing products between the individual frequency components of the spectrum. The spectral regrowth leads to adjacent channel interference.

### 5. BER performance

The BER performance of the wavelet modulation and the OFDM systems is evaluated using the parameters illustrated in Table 2. The achieved performance for other values of  $L$  ( $L \in \llbracket 1, 7 \rrbracket$ ) is similar to that of the studied case  $L = 1$ , with a slight BER degradation in a frequency-selective channel.

#### 5.1. AWGN and flat fading channel

In this part, a comparison between the BER of OFDM, the Dmey wavelet and the Daubechies-20 wavelet for AWGN and flat fading channels, is presented in Fig. 16. Since these are all orthonormal waveform sets, it is only to be expected that

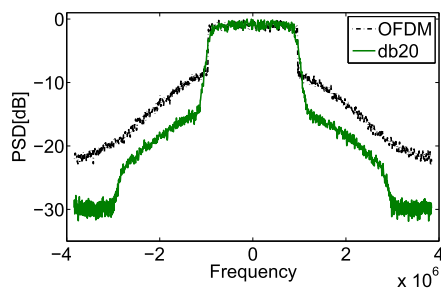


Fig. 14. PSD Comparison between Daubechies-20 wavelet modulation and OFDM at the output of the power amplifier of the Saleh model.

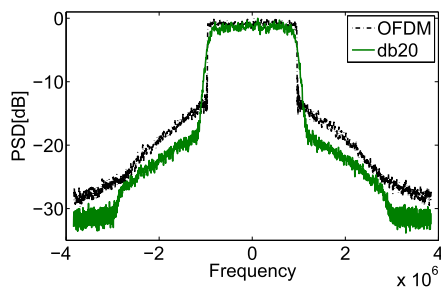


Fig. 15. PSD Comparison between Daubechies-20 wavelet modulation and OFDM at the output of the power amplifier of the Rapp model.

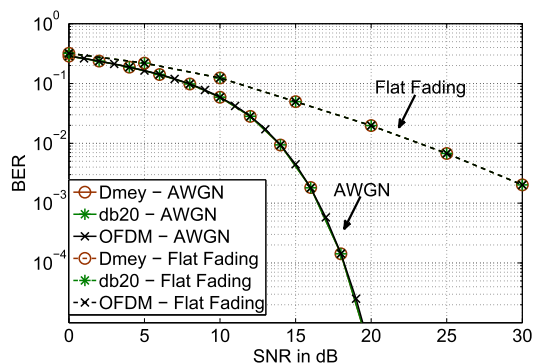


Fig. 16. BER performance comparison for MMSE equalizer in AWGN and flat fading channels.

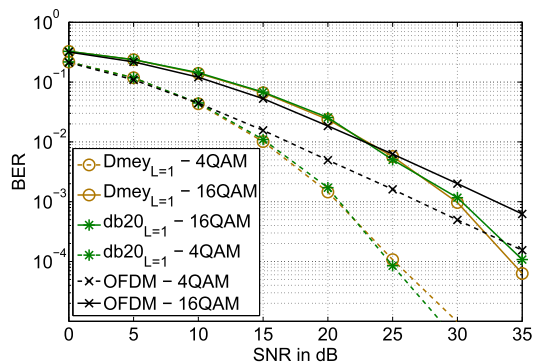


Fig. 17. BER performance comparison for MMSE equalizer in a frequency selective channel.

**Table 2**  
Simulation parameters.

Parameters	Definition	Values
$M$	Number of carriers	128
$S$	Number of frames	100
SNR	Signal to Noise Ratio in dB	0:5:30 and 0:5:35
$n_{\text{loop}}$	Number of iteration loops	100,000
$\Delta F$	Inter-carrier spacing	15 kHz
$L$	Effective number of scales considered	1
CP	Cyclic prefix	25%

**Table 3**  
Channel delay and power profile of ETU channel for LTE standard.

Discrete delay [ns]	0	50	120	200	230	500	1600	2300	5000
Average path gains [dB]	−1.0	−1.0	−1.0	0.0	0.0	0.0	−3.0	−5.0	−7.0

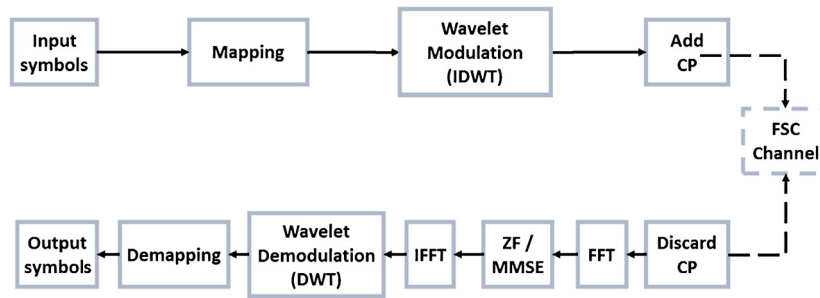


**Fig. 18.** Wavelet transmission chain in a frequency selective channel.

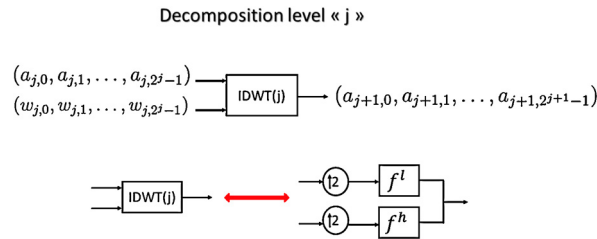


**Fig. 19.** IDWT( $j$ ) implementation.

the performance of all of them will be the same. The simulations confirm that wavelet modulation is as good as OFDM in terms of BER performance.

## 5.2. Frequency selective channel

In a frequency-selective fading channel, a cyclic prefix is added in the time domain to the transmitted signal based on wavelet modulation, and a frequency domain equalization is performed at the receiver side using either the zero forcing (ZF) equalizer or the minimum mean-square error (MMSE) equalizer as presented in Fig. 18. For OFDM, ZF equalizer or MMSE equalizer is used after the FFT demodulation.

The extended typical urban (ETU) model for LTE multipath channel standard [14], defined by the channel delay and the power profile in Table 3, is used in this section. As depicted in Fig. 17, wavelet modulation based on the Dmey wavelet and the Daubechies-20 wavelet reaches a gain of 6.5 dB in terms of SNR for a BER of  $10^{-3}$  and the 4-QAM constellation, compared with OFDM. For higher constellations (16-QAM) and for low SNR values, the performance of OFDM is comparable to that of wavelet modulation. Starting from SNR = 25 dB, wavelet modulation outperforms OFDM.

It is important to highlight that when using channel coding techniques, the gain in terms of SNR will be less significant and will depend also on the efficiency of the coding technique implemented. We have chosen not to use coding to evaluate only the effect of the modulation scheme on the BER performance.

**Table 4**

Number of non-zero coefficients for different wavelet filters.

Wavelet name	Haar	Daubechies-3	Dmey	Daubechies-20
Parameter $K$	2	6	47	30

## 6. Complexity of implementation

### 6.1. Implementation

In order to implement the wavelet modulation system expressed in (8), we apply the Mallat algorithm [9]. For a wavelet modulation signal based on the wavelets of  $L$  scales and the scaling functions of the scale  $J - L$ , the IDWT( $j$ ) should be performed  $L$  times.  $L$  can be also be interpreted as the number of decomposition levels. Let  $\mathbf{C}_n$  be a vector of  $M$  input complex symbols  $C_{m,n}$ . The  $2^{J-L}$  first  $C_{m,n}$  symbols correspond to the  $2^{J-L}$  scaling coefficients  $(a_{J-L,q})_{q \in \llbracket 0, 2^{J-L}-1 \rrbracket}$ . The second  $2^{J-L}$  complex symbols correspond to the wavelet coefficients  $(w_{J-L,k})_{k \in \llbracket 0, 2^{J-L}-1 \rrbracket}$  of the first scale  $J - L$ . First, one IDWT( $j$ ) is performed, which gives in its output  $2^{J-L+1}$  scaling coefficients. After that, the next  $2^{J-L+1}$  coefficients from the vector  $\mathbf{C}_n$  are extracted and considered as wavelet coefficients, and the second IDWT( $j$ ) is performed. The next symbols are processed in the same way until the last scale  $j = J - 1$  is reached. The vector  $\mathbf{C}_n$  can be expressed then as:

$$\begin{aligned} \mathbf{C}_n = & (a_{J-L,0}, a_{J-L,1}, \dots, a_{J-L,2^{J-L}-1}) \bullet (w_{J-L,0}, w_{J-L,1}, \dots, w_{J-L,2^{J-L}-1}) \\ & \bullet (w_{J-L+1,0}, w_{J-L+1,1}, \dots, w_{J-L+1,2^{J-L+1}-1}) \bullet \dots \bullet (w_{j,0}, w_{j,1}, \dots, w_{j,2^j-1}) \\ & \bullet \dots \bullet (w_{J-1,0}, w_{J-1,1}, \dots, w_{J-1,2^{J-1}-1}) \end{aligned} \quad (13)$$

The symbol  $\bullet$  in (13) stands for the concatenation operator. Fig. 19 defines the implementation of one decomposition level  $j$ . According to the Mallat algorithm, the IDWT( $j$ ) consists in upsampling by a factor of two and filtering the approximation coefficients (scaling coefficients) and the detail coefficients (wavelet coefficients), respectively, by a low-pass  $f^l$  and a high-pass  $f^h$  filter, whose responses are derived from the wavelet considered.

### 6.2. Complexity

Since wavelet modulation needs two more blocks (IDWT, DWT) compared with OFDM, as presented in Fig. 18, its complexity is therefore higher than that of OFDM. Let us compute the complexity of the wavelet modulation (IDWT) and wavelet demodulation (DWT) blocks. According to the Mallat Algorithm [9], IDWT( $j$ ) consists in upsampling by a factor of two and filtering the approximation coefficients  $a_{j,k}$  (scaling coefficients) and the detail coefficients  $w_{j,k}$  (wavelet coefficients), respectively, by a low-pass filter  $f^l$  and a high-pass filter  $f^h$ . Let  $K$  be the length of the filters  $f^l$  and  $f^h$  ( $K$  non-zero coefficients). Wavelet modulation is calculated with

$$\sum_{j=J-L+1}^J 2^j K \leq \sum_{j=1}^J 2^j K = 2MK \quad (14)$$

The complexity order in terms of the number of additions and multiplications is therefore  $\mathcal{O}(MK)$ . Knowing that the complexity order of the FFT or the IFFT is  $\mathcal{O}(M \log_2(M))$ , the complexity increase order is about  $\mathcal{O}(\frac{K}{\log_2(M)})$ , which is affordable since  $K$  is bounded, and the number of carriers  $M$  is usually large.

The numbers of non-zero coefficients  $K$  for each one of the wavelets studied in this work are displayed in Table 4. The Haar wavelet has the smallest complexity, but, as we have seen in Section 3, it has the worst PSD. The Dmey wavelet is computationally more demanding than the Daubechies-20 wavelet, but it outperforms the Daubechies-20 wavelet in terms of PAPR, while having the same BER performance. The choice between the Dmey wavelet and the Daubechies wavelet is subject to the PAPR performance required and the complexity of implementation tolerated.

## 7. Conclusion

Wavelet modulation has been proposed in this paper as an alternative modulation with low energy consumption. Based on simulation results, we have shown that wavelets achieve better PAPR performance than OFDM. The Haar wavelet reaches the best PAPR performance, but it suffers from poor spectral characteristics. The Dmey and the Daubechies-20 wavelets have been proposed as wavelets that provide the best trade-off. The properties of wavelet modulation have been compared with those of uncoded OFDM. We have shown that OFDM suffers from a spectral regrowth larger than that of wavelet modulation, while introducing the transmitted signal into a power amplifier. While maintaining the same BER performance in the AWGN channel and the flat fading channel, the variant  $L = 1$  ( $J = 7$ ,  $M = 128$ ) of the wavelet modulation outperforms uncoded OFDM in the frequency-selective channel by up to 6.5 dB, at BER of  $10^{-3}$ , for the MMSE equalizer and the 4-QAM constellation. However, wavelet modulation requires more implementation complexity. The choice of the suitable wavelet

depends on the application, and is subject to trade-off PAPR and spectral efficiency (Haar vs. Dmey), and to trade-off PAPR and complexity of implementation (Dmey vs. Daubechies-20).

Our future work will be to study a suitable channel coding for wavelets to compare its performance with that of Coded-OFDM under a frequency-selective channel. A less complex equalization as well as pilot insertion methods for wavelet modulation are also open subjects to be investigated.

## Acknowledgements

This work has received financial support from the French Government granted to the CominLabs excellence laboratory and managed by the French National Research Agency in the “Investissements d’Avenir” program under reference No. ANR-10-LABX-07-01. The authors would also like to thank the ‘Région Bretagne’, France, for supporting this work.

## References

- [1] M. Chafii, J. Palicot, R. Gribonval, La modulation en ondelettes: une modulation alternative à faible consommation d’énergie, in: Journées Scientifiques 2016 d’URSI-France, Télécom Paris-Tech, Rennes, France, 15–16 March 2016.
- [2] M. Chafii, Y.J. Harbi, A.G. Burr, Wavelet-OFDM vs. OFDM: performance comparison, in: 23rd International Conference on Telecommunications, ICT 2016, Thessaloniki, Greece, 16–18 May 2016, pp. 1–5.
- [3] H. Bogucka, A. Conti, Degrees of freedom for energy savings in practical adaptive wireless systems, *IEEE Commun. Mag.* 49 (6) (2011) 38–45.
- [4] M. Chafii, J. Palicot, R. Gribonval, Closed-form approximations of the peak-to-average power ratio distribution for multi-carrier modulation and their applications, *EURASIP J. Adv. Signal Process.* 2014 (1) (2014) 1–13.
- [5] M. Chafii, J. Palicot, R. Gribonval, F. Bader, A necessary condition for waveforms with better PAPR than OFDM, *IEEE Trans. Commun.* 64 (8) (2016) 3395–3405.
- [6] S. Galli, O. Logvinov, Recent developments in the standardization of power line communications within the IEEE, *IEEE Commun. Mag.* 46 (7) (2008) 64–71.
- [7] S.L. Linfoot, M.K. Ibrahim, M.M. Al-Akaidi, Orthogonal wavelet division multiplex: an alternative to OFDM, *IEEE Trans. Consum. Electron.* 53 (2) (2007) 278–284.
- [8] A. Lindsey, Wavelet packet modulation for orthogonally multiplexed communication, *IEEE Trans. Signal Process.* 45 (1997) 1336–1339.
- [9] S. Mallat, *A Wavelet Tour of Signal Processing*, Academic Press, 2008.
- [10] Y. Meyer, Principe d’incertitude, bases hilbertiennes et algèbres d’opérateurs, in: Séminaire Bourbaki, vol. 28, 1985, pp. 209–223.
- [11] H. Nikoogar, *Wavelet Radio: Adaptive and Reconfigurable Wireless Systems Based on Wavelets*, Cambridge University Press, Cambridge, UK, 2013.
- [12] A.A. Saleh, Frequency-independent and frequency-dependent nonlinear models of TWT amplifiers, *IEEE Trans. Commun.* 29 (11) (1981) 1715–1720.
- [13] C. Rapp, Effects of HPA-nonlinearity on a 4-DPSK/OFDM-signal for a digital sound broadcasting signal, in: ESA, Second European Conference on Satellite Communications (ECSC-2), vol. 1, 1991, pp. 179–184 (SEE N92-15210 06-32).
- [14] ETSI TS 136 101 V8.23.0 (3GPP TS 36.101 V8.23.0 Release 8).